Rock and Soil Mechanics

Volume 43 | Issue 7 Article 2

9-20-2022

Macroscopic and microscopic experimental study on fractal fragmentation characteristics of calcareous sand during one-dimensional compression creep

Bin CHEN
Hunan Provincial Key Laboratory of Geomechanics and Engineering Safety, Xiangtan University, Xiangtan , Hunan 411105, China

Jian DENG
College of Civil Engineering and Mechanics, Xiangtan University, Xiangtan, Hunan 411105, China

Jie-ming HU
College of Mechanics and Materials, Hohai University, Nanjing, Jiangsu 210098, China,
hujiemingxut@163.com

Jian-lin ZHANG
College of Civil Engineering and Mechanics, Xiangtan University, Xiangtan, Hunan 411105, China

See next page for additional authors

Custom Citation

CHEN Bin, DENG Jian, HU Jie-ming, ZHANG Jian-lin, ZHANG Tao, . Macroscopic and microscopic experimental study on fractal fragmentation characteristics of calcareous sand during one-dimensional compression creep[J]. Rock and Soil Mechanics, 2022, 43(7): 1781-1790.

Macroscopic and microscopic experimental study on fractal fragmentation characteristics of calcareous sand during one-dimensional compression creep

Authors
Bin CHEN, Jian DENG, Jie-ming HU, Jian-lin ZHANG, and Tao ZHANG

Rock and Soil Mechanics 2022 43(7): 1781−1790 ISSN 1000−7598
https: //doi.org/10.16285/j.rsm.2021.6723 rocksoilmech.researchcommons.org/journal

Macroscopic and microscopic experimental study on fractal fragmentation characteristics of calcareous sand during one-dimensional compression creep

CHEN Bin[1, 2], DENG Jian[1], HU Jie-ming[1, 3], ZHANG Jian-lin[1], ZHANG Tao[1]

1. College of Civil Engineering and Mechanics, Xiangtan University, Xiangtan, Hunan 411105, China
2. Hunan Provincial Key Laboratory of Geomechanics and Engineering Safety, Xiangtan University, Xiangtan , Hunan 411105, China
3. College of Mechanics and Materials, Hohai University, Nanjing, Jiangsu 210098, China

Abstract: Calcareous sand is a natural foundation material for ports, airports and some civil buildings in ocean areas. Through the one-dimensional compression creep test of calcareous sand and the analysis of its micro-structure, it was found that the surface pore area decreased after creep and showed a dispersed distribution. In addition, the characteristics of instantaneous deformation, rapid deformation and attenuation deformation of the sample during the test were highly correlated with the particle size. The relative particle breakage rate and mass fractal dimension improved based on fractal theory were used to describe the degree of particle breakage after creep. The relationship between the decay of fractal dimension and creep with time, as well as the linear relationship between the fractal dimension of macroscopic mass and the fractal dimension of microscopic surface was obtained. On this basis, the fractal fracture behavior of calcareous sand with a single particle size group during long-term creep was analyzed at multiple scales, and the corresponding macro and micro cross-scale correlation was studied. The development of particle breakage and the variation of microscopic pores during creep were obtained. This study proved the rearrangement, crushing and grinding behavior of calcareous sand particles in the creep process, and revealed the creep mechanism of calcareous sand.

Keywords: calcareous sand; creep; particle breakage; macro-micro analysis; creep mechanism

1 Introduction

"Long term stability" is one of the key issues in China's Island and reef engineering construction [1−2]. Calcareous sand is a natural foundation material for island and reef construction projects, but its particle shape is irregular, rich in pores, low strength and easy to be broken [3−6]. Moreover, the physical and mechanical properties of calcareous sand are very different from those of terrigenous sand [7−8]. On the basis of the existing studies on the creep of sand [9−10], many researchers have carried out research on the creep characteristics of calcareous sand. Ye et al. [1], Sanzeni et al.[11], Lü et al.[12], and Wang et al. [13] found that under a certain load, calcareous sand would produce creep phenomenon with longer duration and larger deformation than terrigenous sand through one-dimensional compression creep test, triaxial drained compression creep test and stress relaxation test with a test period of 1−16 days. As for the creep mechanism of calcareous sand, Lade et al.[14−15], Zhang et al.[16], Wang et al.[17] and Xiao et al.[18] found that creep of calcareous sand was related to particle rearrangement and particle breakage based on the analysis of triaxial drained compression creep test, one-dimensional compression creep test and particle size distribution test. They demonstrated that the creep of calcareous sand was mainly caused by the sliding of fine particles generating from particle breakage to fill the pores. At the initial loading stage, the degree of particle breakage and sample volume changed significantly with time, and the response trends of particle breakage with time and stress were similar. Through one-dimensional compression test and ring shear test, Coop et al.[19], Shen et al.[20], and Miao et al. [21] found that the particle breakage of granular materials tended to a self-similar fractal distribution, and it was closely related to the rate of particle breakage. Due to the particularity of the creep characteristics and creep mechanism of calcareous sand, Zhang et al.[22] and Zhang et al.[23] described the particle breakage behaviors by using fractal dimension and carried out research on the characteristics of particle breakage and morphology change during creep.

Based on the relative particle breakage rate (B_{rE}) redefined by Einav[24] and the modified fractal model, this paper describes the evolution of particle size distribution (PSD) of calcareous sand at different times during one-dimensional compression creep test

Received Date: 12 December 2021 Revised: 28 March 2022
This work was supported by the Special Project for the Construction of Innovative Provinces in Hunan Province (2019RS1059) and the National Natural Science Foundation of China (51774131, 41972282).
First author: CHEN Bin, male, born in 1977, PhD, Associate Professor, PhD supervisor, mainly engaged in research work on geological disaster prevention and
Corresponding author: HU Jie-ming, male, born in 1996, PhD candidate, majoring in marine geotechnical engineering. E-mail: hujiemingxut@163.com

and the evolution of some microscopic parameters, such as such as particle porosity, before and after creep. Moreover, based on the fractal theory, the creep mechanism of calcareous sand was analyzed from the macro and micro perspectives in this study, which further revealed and clarified the creep mechanism.

2 Materials and testing methods

2.1 Basic properties of samples

The calcareous sand samples in this study were collected from a reef island in the South China Sea. They were grayish white uncemented loose marine clastic sediments with a calcium carbonate content of 96.51%. The basic physical parameters of the calcareous sand sample are shown in Table 1.

Table 1 Basic physical parameters of the calcareous sand sample

d_{10} /mm	d_{30} /mm	d_{60} /mm	C_u	C_c	Specific gravity	Maximum dry density /(g • cm^{-3})	Minimum dry density /(g • cm^{-3})
0.14	0.24	0.36	2.57	1.14	2.77	1.56	1.29

Notes: d_{10}, d_{30} and d_{60} are the effective particle size, continuous particle size and limited particle size respectively; C_u and C_c are the coefficient of uniform and curvature coefficient, respectively.

The sample was mainly composed of particles with a particle size of 0.25−0.5 mm (56.24% by mass) and poor grading. The curvature coefficient C_c is 1.14, satisfying C_c =1−3, and the coefficient of uniformity C_u is 2.57, smaller than 5.

According to the "*Standard for soil test method* " (GB/ T50123−2019) [25]: "The maximum particle size should be smaller than 1/10 of the sample diameter." In this study, after removing irregular particles with particle sizes larger than 5 mm, there were still some particles with large size differences in the three-dimensional directions, such as dendritic and spindly-cone particles. In order to reduce the effect of particle shape on the test results, the samples were divided into three single uniform particle size groups (as shown in Fig.2) of 0.25−0.50 mm (fine sand), 0.5−1.0 mm (medium sand) and 1.0−2.0 mm (coarse sand) for comparative test combined with the particle gradation state of complex particle size group deduced and calculated by Tong et al.[26] and Lin et al.[27] according to the single particle size group. By controlling the falling height and falling rate, according to the pre-test results, the sand falling method was used to prepare the samples from three different particle size groups in layers with three dry densities of 1.244, 1.158 and 1.145 g/cm^3, respectively.

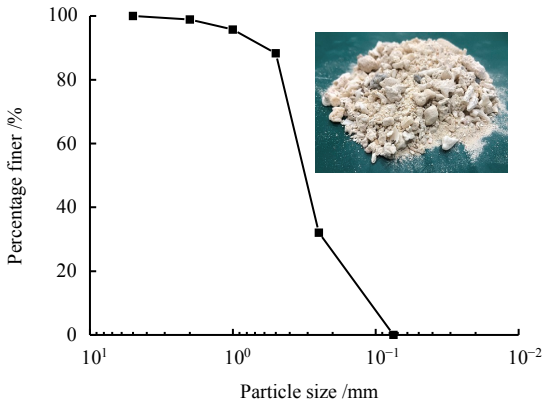

Fig. 1 The calcareous sand sample and its grading curves

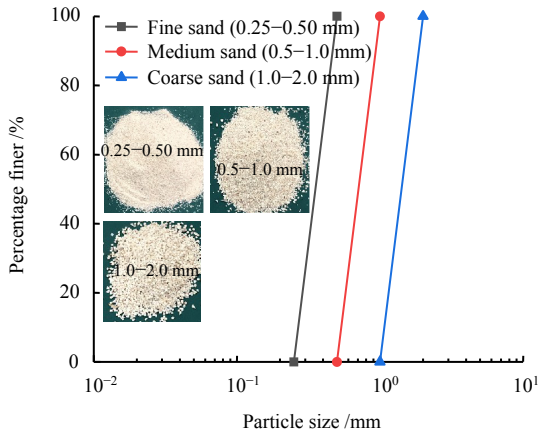

Fig. 2 Particle size distribution curves of test materials

2.2 Testing program of macroscopic creep test

Wargaming (WG) type single lever triple high-pressure oedometer produced by Nanjing Soil Instrument Factory was used for dimensional compression creep tests. The diameter and the height of the sample tested was 61.8 mm and 20 mm, respectively. The test adopted weight to load step by step, and the vertical stress was 50, 100, 200, 400 and 800 kPa, respectively. When the axial deformation was smaller than 0.005 mm for 5 consecutive days, the creep test was considered to be complete. The specific testing scheme is shown in Table 2.

Table 2 Creep test scheme for calcareous sand

Particle size /mm	Relative density /%	Maximum void ratio	Minimum void ratio	Stress level /kPa	Creep time /d
0.25−0.50	30	1.40	0.88	50,100,200,400, 800	2,7,14, 25,56
0.5−1.0	30	1.52	1.05	50,100,200,400, 800	2,7,14, 25,56
1.0−2.0	30	1.58	1.07	50,100,200,400, 800	2,7,14, 25,56

2.3 Microstructure analysis

Through digital image technology[28−29], the surface images of soil samples at different times of creep were

compared to study the evolution of particle breakage and the variation of microstructure of the calcareous sand before and after creep. The optical camera system used a digital camera with a 12-megapixel CMOS image sensor. The fixed camera height was 20 cm from the sample surface, and the method of center imaging was employed to photograph the compression surface of the sample at different times. The images were processed by the software Image-Pro Plus 6.0 (IPP6.0) to obtain the porosity and the basic parameters of particle dimension of the sample compression surface. In combination with the macro and micro research methods of sand particle breakage in the previous literatures[30−33] and the built-in measurement tools of IPP software, surface porosity, particle equivalent area and particle equivalent perimeter were selected as basic particle dimension parameters. The definitions of these parameters are shown in Table 3.

Table 3 Basic particle size parameters

IPP Name	Symbol	Definition
Equivalent area	A	Average area of the convex polygons connected by points on the outermost contour of particles
Equivalent perimeter	P	Average perimeter of the convex polygons connected by points on the outermost contour of particles

3 Analysis of creep test results

3.1 Creep characteristics of calcareous sands

From creep curves of particles of different particle size groups under different stress conditions (see Fig.3), three deformation stages of the calcareous sand, i.e., instantaneous deformation stage, rapid deformation stage and stable creep attenuation deformation stage can be identified under one-dimensional compression. Instantaneous deformation occurred at the moment of loading, and the instantaneous deformation accounted for 26%−70% of the total deformation, and it was mainly compression deformation. Then with the increase of time, the sample entered the rapid deformation stage (the axial strain rate was higher than 0.005 mm/d), and the deformation at this stage accounted for 23%−59% of the total deformation. After that, the sample entered the creep attenuation deformation stage, in which the deformation only accounted for less than 18% of the total deformation, and the deformation finally tended to be stable. Under the same stress condition, with the increase of stress, the axial strain of the samples of different particle size groups increased and showed a significant difference: although the difference in dry density between the calcareous sands with particle sizes of 0.25−0.50 mm and 0.5−1.0 mm was 0.086 g/cm^3, with the increase of stress, the difference in axial strain between them increased from 0.03% to 1.17%, gradually widening the gap. The same phenomenon can be observed between the calcareous sands with particle sizes of 0.5−1.0 mm and 1.0−2.0 mm: the difference in dry density between the two groups of samples was only 0.013 g/cm^3, but the difference in axial strain increased from 0.15% to 3.03%. It can be concluded that the particle size had a considerable influence on the compression deformation of calcareous sand.

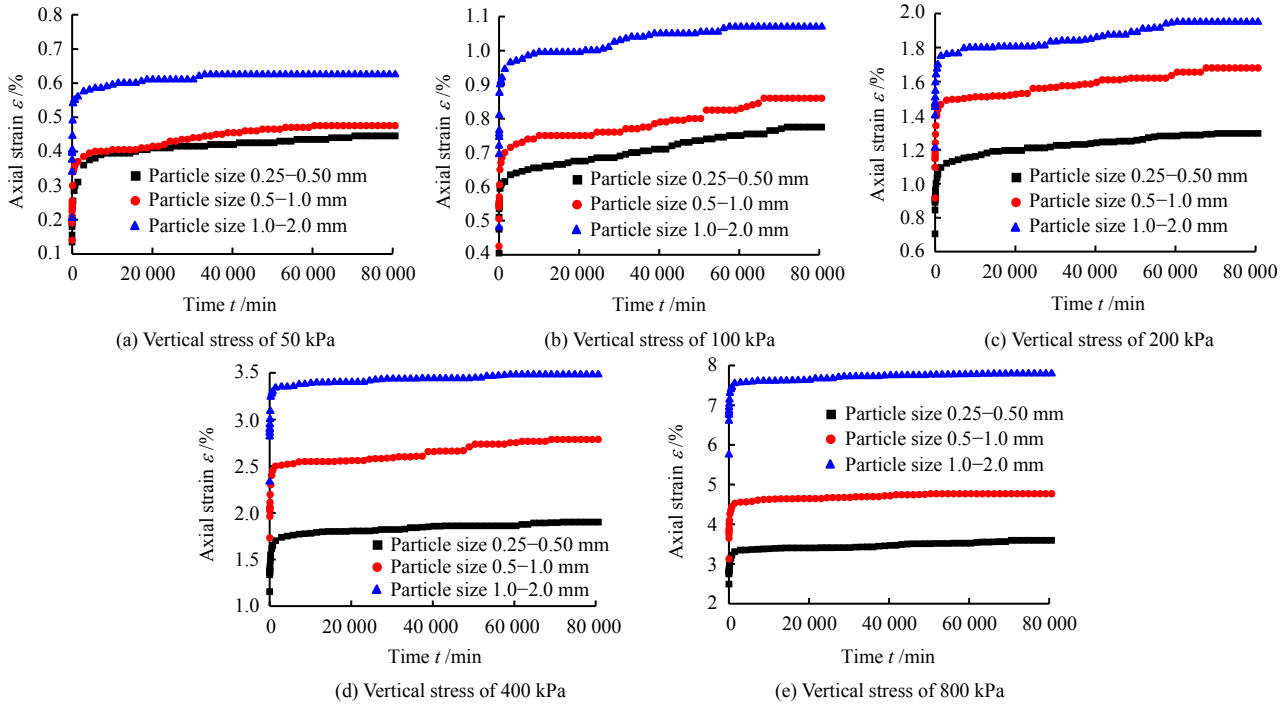

Fig. 3 Curves of axial strain−time during creep of calcareous sand under different vertical stresses

At a lower stress level, the axial deformation of calcareous sand in the 0.25−0.5 mm and 0.5−1.0 mm particle size groups was small and similar, while the axial deformation of calcareous sand in the 1.0−2.0 mm particle size group was large. This is because the larger the particle size of calcareous sand, the more distinct the edges and angles, the more complex the particle shape[34], and the smaller the strength for particle breakage[35]. The calcareous sand sample with particle sizes of 1.0−2.0 mm had larger initial porosity and smaller strength for particle breakage, resulting in larger deformation of particle rearrangement and a small part of particle breakage deformation at a lower stress level. The calcareous sand samples with particle sizes of 0.25−0.50 mm and 0.5−1.0 mm had smaller particle size, smaller shape difference, larger strength for particle breakage, and similar relative density. At a lower stress level, the axial deformation of them mainly came from the rearrangement of particles. With the increase of stress level, the particle rearrangement and the degree of particle breakage of the sample further increased. At this moment, the difference of particle size, particle shape and the strength for particle breakage indirectly resulted in the difference of the axial strain deformation of the samples with different particle sizes.

From the response curve of axial strain rate to time (by week) (see Fig.4), it can be seen that the rapid deformation stage occurred after instantaneous deformation stage, and the axial strain rate decreased rapidly with the increase of time. On the 14th day, the rapid deformation stage was basically completed, and the minimum deformation rate was 4.29×10^{-4} mm/d. At the stable creep attenuation deformation stage, the axial strain rate converged and gradually approached 0.

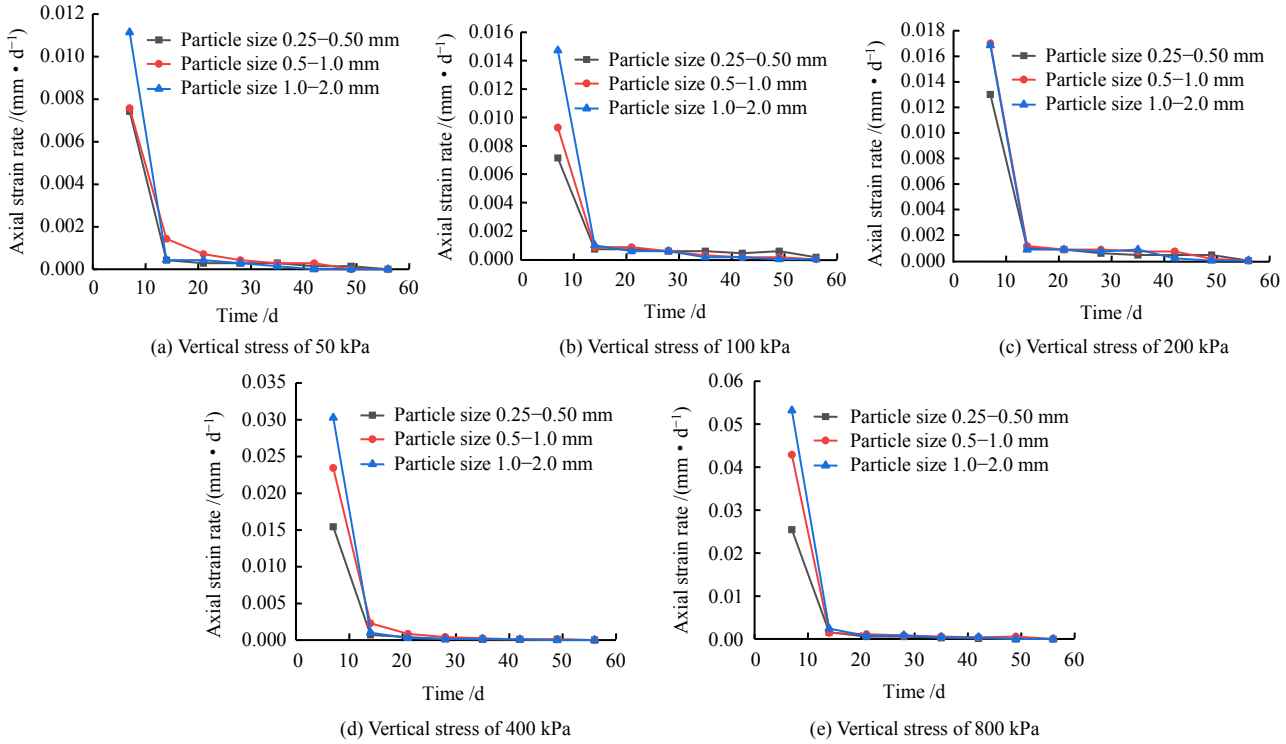

Fig. 4 Curves of axial strain rate−time during creep of calcareous sand under different vertical stresses

As shown in Fig.4, under the same vertical stress level, the axial strain rate of the calcareous sand samples with larger particle sizes was slightly higher than that of the calcareous sand samples with smaller particle sizes at the rapid deformation stage. However, at the creep attenuation deformation stage, the strain rate of the three groups of calcareous sands with different particle sizes tended to be stable, indicating that the particle size affected the axial strain rate at the creep stage. By comparing the curves under different vertical stress levels, it can be seen that the extreme value of the axial strain rate gradually increased with the increase of stress level, from 0.011 mm/d to 0.053 mm/d, indicating that the stress level was closely related to the axial strain rate of calcareous sand during compression deformation.

3.2 Fractal behaviour of particle breakage

To avoid the damage and secondary breakage of the particles caused by the vibrating screen machine, affecting the test results, this paper adopted the method of manually vibrating the sieves slowly and continuously for 15 minutes to obtain the remaining mass of the sieve

tray at all levels, and the PSD curve of each particle size group after particle breakage under different vertical stress levels was plotted in the double logarithmic coordinate axis (see Fig. 5).

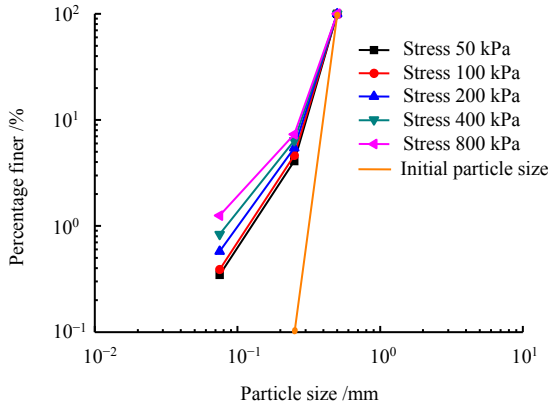

(a) Calcareous sand with a particle size of 0.25−0.50 mm

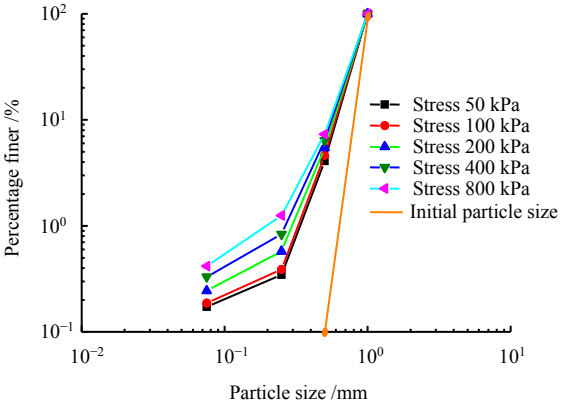

(b) Calcareous sand with particle size of 0.5−1.0 mm

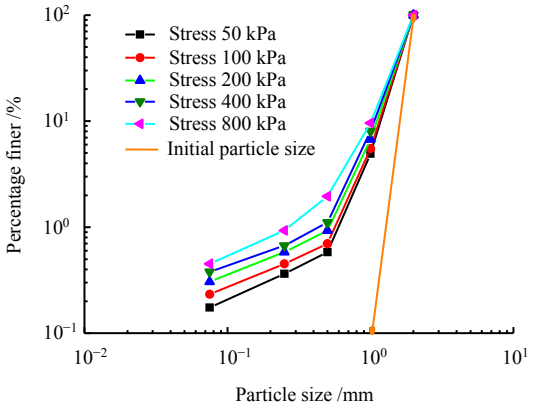

(c) Calcareous sand with a diameter of 1−2 mm

Fig. 5 PSD evolution of calcareous sand during creep (double logarithmic axes)

Figure 5 shows that the PSD curves of calcareous sands of all particle size groups are similar in shape and are all concave curves. Through comparative analysis of PSD curves of calcareous sands of different particle size groups, it can be found that with the increase of particle size, the range of particle size distribution increased from 0.075−0.500 mm to 0.075−2.000 mm, and the curve was transitioned from a locally simple steep curve to gradual curves with multiple particle size groups. This indicated that the particle breakage of calcareous sand was developing towards the state of ultimate particle distribution and had ductility. By comparing the PSD curves of calcareous sands from the same particle size group, with the increase of stress level, the PSD curve took it was observed that the initial particle size distribution curve as the baseline, rotated clockwise and gradually became concave and then tended to be flat, showing that the particle breakage rate of calcareous sand increased, and the self-similarity was highly consistent.

The PSD fractal model proposed by Tyler et al. [36], which is expressed by the relationship between cumulative particle mass and particle size, was used to process the PSD curve to obtain the mass fractal dimension D.

$$\frac{M\left(r<d_i\right)}{M_{\mathrm{T}}}=\left(\frac{d_i}{d_{\mathrm{M}}}\right)^{\alpha} \tag{1}$$

where r is the size of the selected particle; d_i is the sieve aperture of the i-th layer of screening, and the minimum and maximum particle sizes of soil particles are assumed to be d_{m} and d_{M}, respectively; M ($r<d_i$) is the cumulative mass of particles with a particle size smaller than d_i (it is consistent with the commonly used PSD curve); M_{T} is the total mass of particles; $\alpha=3-D$, D is the fractal dimension, ranging from 0 to 3.

The relative particle breakage rate B_{rE} (as shown in Fig. 6) proposed by Einav et al. [24] based on fractal theory was used to describe the degree of particle breakage during creep. The area nclosed by the initial PSD curve and the ultimate particle size cutoff line is defined as the crushing potential B_{p}. The area enclosed by the initial PSD curve, the PSD curve after particle breakage and the cutoff line of the ultimate particle size is defined as the total breakage amount B_{t}. The ratio of the two is defined as the relative particle breakage rate B_{rE}, used for measuring the degree of particle breakage. The value of B_{rE} can be calculated according to the following equation:

$$B_{\mathrm{rE}}=\frac{B_{\mathrm{t}}}{B_{\mathrm{p}}} \tag{2}$$

The one-dimensional compression creep test where the sample creeped 2, 7, 14, 28 and 56 days under the stress of 800 kPa is selected as an example, and the response of mass fractal dimension D of calcareous sand with different particle size groups to time in the whole creep process is plotted in Fig. 7. The correlation between the relative particle breakage rate B_{rE} and mass fractal dimension D during the creep is shown in Fig. 8.

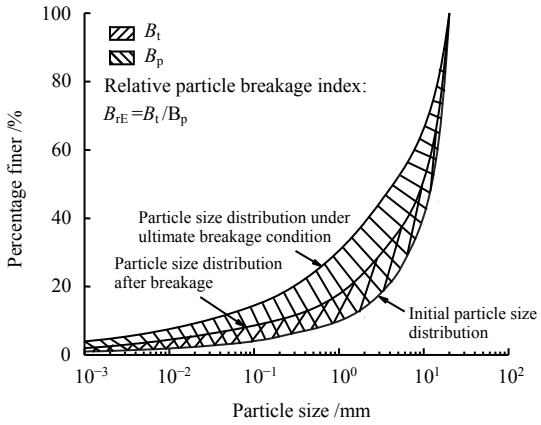

Fig. 6 Relative particle breakage rate B_{rE}

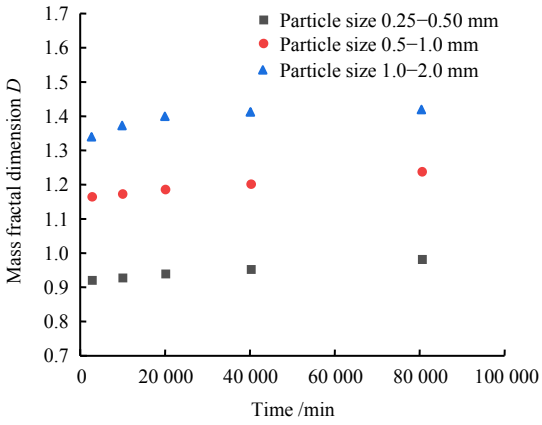

Fig. 7 Response of mass fractal dimension of calcareous sand samples with different particle sizes to time

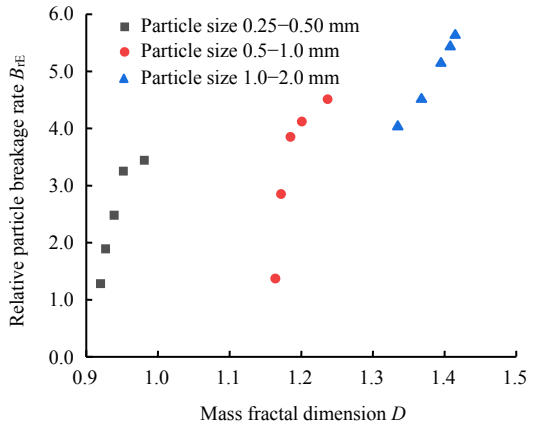

Fig. 8 Response of particle breakage to mass fractal dimension during creep of calcareous sand

As can be seen from Fig. 7, influenced by the loading stress level, the variation tendency of mass fractal dimension D with creep time was a slow increase as a whole with a small increment. Since the change of mass fractal dimension of samples of each particle size group during creep was small, it was difficult to observe the development trend. So, the incremental change of mass fractal dimension D after 2, 7, 14, 28 and 56 days of creep, namely the average growth rate, was selected for analysis. For these different particle size groups, the average growth rate of D of particle size group with 0.25−0.50 mm was similar to that in the 0.5−1.0 mm particle size group, lying in the range of 0.001 0−0.001 5/d. However, the average growth rate of D of the particles in the 1.0−2.0 mm particle size group decreased from 0.006 6/d within the 2−7 days of creep to 0.000 25/d at the later stage of creep, showing an obvious decreasing trend. By combining the knowledge that the larger the particle size of the calcareous sand sample, the larger the mass fractal dimension, it can be concluded that the larger the particle size, the higher the degree of particle breakage.

Due to the small stress level, although particle breakage cannot be ignored in the creep process of calcareous sands in different particle size groups, it was far from reaching the ultimate state of fractal breakage and it has been in the development process of fractal breakage, so the mass fractal dimension D continued to increase slightly.

The deformation of each sample in the creep test includes two stages: rapid loading deformation stage and creep deformation stage [1], in which the sample enters the creep deformation stage after 2 days of one-dimensional compression. Therefore, the increment between each time point in the creep deformation stage was selected to characterize the creep characteristics, and the changing trend of the increment between points can be expressed by the change of the increment rate. It can be seen from Fig.8 that with the increase of time, the relative particle breakage rate B_{rE} and the mass fractal dimension D of calcareous sand increased correspondingly. The increase rate of B_{rE} of the particles in the 0.25−0.50 mm particle size group gradually slowed down from 0.122 %/d to 0. 0.006 %/d; the increase rate of B_{rE} of the particles in the 0.5−1.0 mm particle size group gradually decreased from 0.296 %/d to 0.014 %/d. However, for the particles in the 1.0−2.0 mm particle size group, the B_{rE} was 4.03% in the early stage, so the increase rate in the later stage only changed from 0.096 %/d to 0.007 %/d. The response of B_{rE} to D for the samples in each particle size group was relatively similar, that is, it increased with the increase of D. Both D and B_{rE} of calcareous sand samples with coarse particles are larger than those with fine particles, indicating that the particle breakage modes of coarse particles and fine particles are different in the whole breakage process.

By combining the change of the PSD curves before and after the test (see Fig. 5), the samples with 56 days of creep at 800 kPa were taken as an example for analysis. For the particles in the 0.25−0.50 mm particle size group, after the test, the mass of the particles with a size of 0.075−0.250 mm accounted for 2.98%, and the mass of the particles with a size smaller than 0.075 mm accounted for 1.32%. For the particles in the 0.5−1.0 mm particle size group, after the test, the

mass of the particles with a size of 0.25−0.50 mm accounted for 6.06%, and the mass of the particles with a size smaller than 0.075 mm accounted for 0.41%. For the particles in the 1.0−2.0 mm particle size group, after the test, the mass of the particles with a size of 0.5−1.0 mm accounted for 7.64%, and the mass of the particles with a size smaller than 0.075 mm accounted for 0.40%. It can be concluded that the larger the particle size, the larger the proportion of the mass of the particles with a size in the next size level produced by breakage, and the smaller the proportion of the mass of the particles with a size smaller than 0.075 mm produced by grinding.

To sum up, both breakage and grinding of calcareous sand particles existed in the creep process. By comparing coarse particles with fine particles, it was inferred that the breakage degree of coarse particles was higher than that of fine particles, and the grinding degree of coarse particles was lower than that of fine particles. Both particle breakage and grinding would continuously increase the relative particle breakage rate and the mass fractal dimension. The changing trends of B_{rE} and D of samples with time for the particles in the different particle size groups were different, indicating that the time response of B_{rE} and D in the process of particle fractal breakage was associated to the particle size of samples.

4 Analysis of microstructure test results

The surface of the sample in the creep test at each time was digitally photographed, and the microscopic image of the sand sample surface was binarized and analyzed by Image Pro Plus to obtain the particle breakage on the surface of the sand sample. Using the measurement tools in IPP software, the surface porosity and the surface fractal dimension were selected to conduct microscopic quantitative analysis of the evolution of particle breakage. At a stress of 800 kPa, the comparison of surface particle breakage and pore development of calcareous sand samples with particle sizes in the three different particle size groups before and after 56 days of creep is shown in Fig. 9.

It can be observed from Figs. 9 (a), 9 (c) and 9 (e) that the surface pore distributions of calcareous sand samples with particle sizes in the different particle size groups before creep were significantly different (white dots represent the surface pores). With the increase of particle size, the surface pores showed different characteristics, and gradually changed from a large number of scattered small pores to a large area of connected pores. The surface pores of the particles in the 0.25−0.50 mm particle size group were small and evenly dispersed. The dry densities of the samples with the particles in the other two groups were not much different, but the surface pore characteristics were still different due to the influence of particle size. The surface pores of the samples with the particles in the 1.0−2.0 mm particle size group were significantly larger than those in the 0.5−1.0 mm particle size group, and the pores were narrow and connected by small channels. By comparing the surface images of the samples with particles in the different particle size groups before creep and after 56 days of creep, it was found that the surface pore area and the surface pore distribution changed remarkably after 56 days of creep. Specifically, the number and area of white dots representing pores were dramatically reduced, and the distribution state changed from dense to relatively loose. This is because large pores would evolve into small pores as the creep progressed, and some of the small pores would gradually disappear. The development of surface pores of the samples with different particle size groups basically conformed to the evolution of particle breakage before and after creep. Due to the long-term action of loading, the sample particles underwent a series of micro-behaviors, such as rearrangement, interlocking, grinding and breakage, leading to creeping deformation. The pores between particles were changed by the remodelling of the interparticle structure, and the particle debris formed by breakage and grinding.

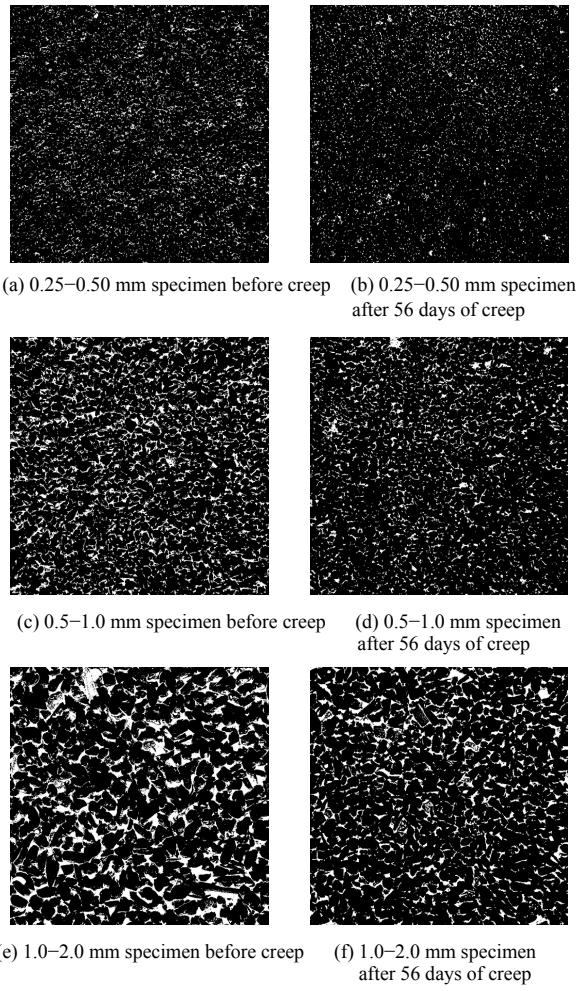

Fig. 9 Binarization diagram of calcareous sand surface before and after creep

During the creep of calcareous sand, there existed the fractal breakage behavior of particles. In order to study the variation of microstructure, interparticle pores and surface fractal dimension, the changes of surface porosity of calcareous sand samples with particles in the different particle size groups before and after 56 days of creep at 800 kPa were plotted in Fig.10, and the response of the microscopic surface fractal dimension with time is shown in Fig. 11.

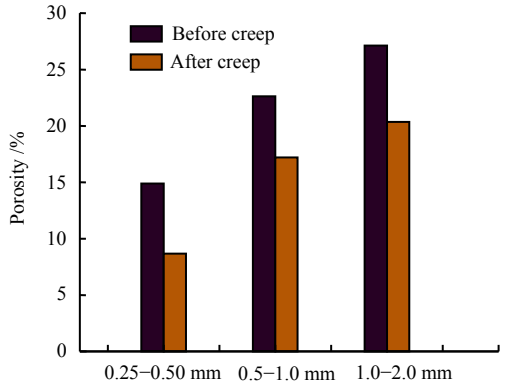

Fig. 10 Porosity of calcareous sand surface before and after creep

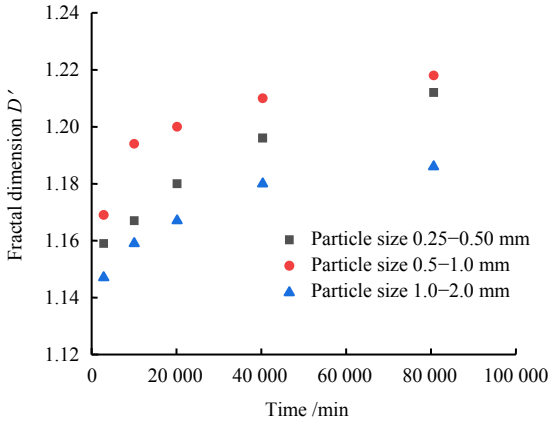

Fig. 11 Response of fractal dimension of calcareous sand surface to time

Figure 10 shows that the surface porosity of calcareous sand samples with different particle sizes decreased after creep. This phenomenon can be explained by the fact that the pores between the irregular particles were filled by the fine particle debris produced by particle sliding and rearrangement, continuous grinding and particle breakage during the creep of the calcareous sand samples with different particle sizes. Therefore, the surface porosity decreased Notably after 56 days of creep. For calcareous sand samples with different particle sizes, the porosity of fine sand samples with the particle size of 0.25−0.50 mm decreased by 41.7%, while the porosities of medium sand samples and coarse sand samples decreased by 23.9% and 24.9%, respectively, almost the same. It suggested that the change of surface porosity before and after creep was closely related to particle size.

The mass fractal dimension obtained from the macro sieving sample reflects the three-dimensional space fractal of the calcareous sand sample in the creep breakage process. In the microstructure test, using the built-in measurement tool of IPP software, the surface fractal dimension reflecting the two-dimensional plane fractal situation of the sample during creep was calculated by means of the box-counting method and the equivalent area and perimeter method. Ye et al. [37] used the surface fractal dimension to describe the morphological changes of soil particles, and the calculation equation is as follows:

$$\lg P = \frac{D'}{2} \times \lg A + C \tag{3}$$

where P is the equivalent perimeter; A is the equivalent area; D' is the fractal dimension; and C is a fitting constant.

As displayed in Fig.11, the fractal characteristics of the microstructure of calcareous sand on the two-dimensional plane during the creep showed an increasing trend of attenuation with time, which was consistent with the variation of the relative particle breakage rate B_{rE} and the mass fractal dimension D with time. As the stress level did not reach the ultimate condition of particle fractal, there would be some differences in surface fractal characteristics, but they were all developing towards the ultimate fractal distribution.

5 Macro and micro correlation analysis

The evolution of particle breakage during the creep of calcareous sand was analyzed by using macroscopic one-dimensional compression creep test and microscopic digital image processing technology. In this study, the relative particle breakage rate (B_{rE}) and the changing magnitude of surface porosity were used as two indicators. The variations of these two indicators before and after 56 days of creep of calcareous sand at 800 kPa are listed in Table 4.

Table 4 Changes of relative particle breakage rate B_{rE} and amplitude of surface porosity after creep

No.	Particle size /mm	Relative particle breakage rate B_{rE} /%	Reduction of calcareous sand surface porosity /%
A	0.25−0.50	3.44	41.7
B	0.50−1.00	4.51	23.9
C	1.00−2.00	5.73	24.9

As can be observed from Table 4, it is obvious that the relative particle breakage rate B_{rE} uniformly increased. with the increase of particle size. By comparing the samples A and B, and C after 56 days of creep, it was found that the changing magnitude of B_{rE} was 1.07 and 1.22, respectively, and the difference in dry density was

0.086 g/cm^3 and 0.013 g/cm^3, respectively. It can be seen that in this range of dry density in this study, the change of dry density had a weak influence on the B_{rE}, and the particle size played a dominant role in the particle breakage in the creep process. At the same time, analyzing the changing magnitude of surface porosity of the samples with different particle size groups demonstrated that the sample group A with large dry density and small particle size had the largest changing magnitude of surface porosity of 41.7%, but B_{rE} was the smallest, indicating that the largest factor affecting the change of surface porosity at this time was the rearrangement of particles. With the decrease of dry density and the increase of particle size, the value of B_{rE} continued to increase, but the changing magnitude of surface porosity was not significant, which was 23.9% and 24.9% respectively. This is because the larger particles can form the skeleton of resistance to external force in a short time, and the degree of particle rearrangement is small. For this reason, particle breakage and grinding play an increasingly important role in the creep process.

Both the surface fractal dimension and the mass fractal dimension are used to describe the fractal characteristics of sand samples in the test. The surface fractal dimension is to analyze and study the change of the particle shape on the surface of the sample from the two-dimensional perspective, and the mass fractal dimension is to analyze and study the evolution of particle size from the three-dimensional perspective. Zhao et al.[38] found in the study on particle breakage characteristics of quartz sand and granite that the small particles generated by particle breakage all met the fractal distribution, indicating that particle breakage had scale invariance. Therefore, whether it is a single particle, a two-dimensional space on the surface of the sample or a three-dimensional space of the sample as a whole, there are specific manifestations of fractal characteristics and particle breakage has scale invariance. Based on this, the relevance of scale invariance of calcareous sand particles in two-dimensional space and three-dimensional space can be further explored.

The cross-scale correlation and multi-scale analysis based on fractal theory (see Fig.12) were carried out based on the response of three-dimensional spatial mass fractal dimension and two-dimensional planar surface fractal dimension with time in the creep test of calcareous sand at 800 kPa stress for 56 days.

It can be seen from Fig.12 that through the cross-scale correlation and multi-scale analysis of the macroscopic mass fractal dimension and the microscopic surface fractal dimension, it was found that the fractal situation of calcareous sand samples with different particle size groups at two scales was highly similar, and the fractal dimensions at different scales were linearly and positively correlated, with high correlation coefficients (R^2>0.92). Comparing the surface fractal dimension of the samples with particles in the different particle sizes groups at the same time point, it can be found that the surface fractal dimension of the samples with the particle size of 0.5−1.0 mm was the largest, followed by that of 0.25−0.50 mm, and that of the samples with the particle size of 1.0−2.0 mm was the smallest, which may be affected by the small stress level and single two-dimensional plane observation. There is no obvious regularity between the surface fractal dimension and the particle size. The mass fractal dimension of the calcareous sand samples with the particle size of 1.0−2.0 mm was larger than that of 0.5−1.0 mm, and the mass fractal dimension of the samples with the particle size of 0.5−1.0 mm was larger than that of 0.25−0.5 mm. That is, the mass fractal dimension of coarse particles was larger than that of fine particles, which was consistent with the finding that the breakage strength of coarse particles was lower than that of fine particles, indicating that under the same stress level, the breakage degree of coarse particles was larger than that of fine particles.

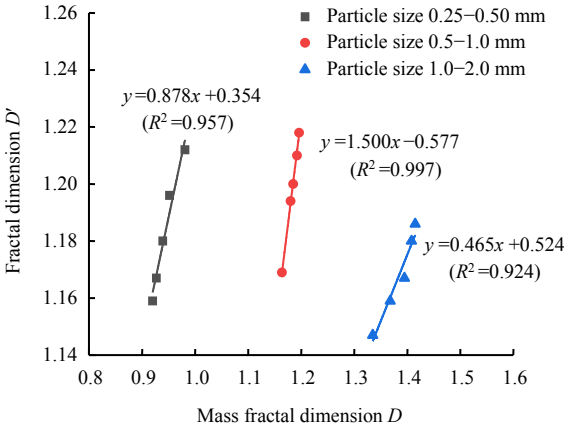

Fig. 12 Fitting of relationship between mass fractal dimension and surface dimension of calcareous sand

Although the fractal dimension of the calcareous sand samples with different particle size groups in the three-dimensional space was larger in the creep process, the tendency of fractal breakage was consistent in both the three-dimensional space on the macro scale and the two-dimensional plane on the micro scale. The fractal dimension gradually increased with the creep time, which indicates that during the creep, particle rearrangement and reorganization, particle slippage and rotation, and particle breakage and grinding occurred, and the special self-similarity was reflected in both macro space and micro plane. Based on fractal theory, the relative particle breakage rate and two kinds of fractal dimensions can be used to describe the creep process of calcareous sand.

6 Conclusions

The fractal breakage characteristics of calcareous sand were studied by one-dimensional compression creep tests under different creep times and stress levels. The image processing software was used to binarize and analyze the surface microstructure of the calcareous sand sample after creep. Based on the macro fractal breakage behaviors and the evolution of microstructure, the cross-scale correlation and multi-scale analysis were carried out to reveal the creep mechanism of calcareous sand. The main conclusions are drawn as follows:

(1) The deformation of calcareous sand samples with particles in different particle size groups included the instantaneous deformation stage, the rapid deformation stage and creep attenuation deformation stage that tends to be stable. In the creep attenuation deformation stage, an obvious stepwise growth can be observed at higher coordinate axis accuracy. During the creep, the fractal breakage behaviors existed, and the evolution of mass fractal dimension D and relative particle breakage rate B_{rE} was closely related to the particle size.

(2) After creep, the porosity of the samples containing each particle size group decreased significantly, and the surface pore area showed a dispersed distribution. Combined with the relative particle breakage rate, it can be found that the fine sand particles with large dry density were dominated by particle rearrangement during creep, while the medium and coarse sand particles with small dry density were dominated by particle breakage and grinding.

(3) The creep process of calcareous sand showed highly similar fractal breakage behaviors at both macro and micro scales. There was a positive linear correlation between the mass fractal dimension and the surface fractal dimension, both of which can be used to describe the creep process of calcareous sand. It can be concluded that the creep mechanism of calcareous sand was closely related to particle rearrangement, particle breakage and grinding, and the development of porosity in combination with the macro and micro test results,

References

[1] YE Jian-hong, CAO Meng, LI Gang. Preliminary study on the creep characteristics of calcareous sand from reclaimed coral reef islands in South China Sea[J]. Chinese Journal of Rock Mechanics and Engineering, 2019, 38(6): 1242−1251.

[2] LI Xiao-mei, WANG Fang, HAN Lin, et al. Experimental study on creep properties of coral sand[J]. Chinese Journal of Geotechnical Engineering, 2020, 42(11): 2124−2130.

[3] ZHU Chang-qi, CHEN Hai-yang, MENG Qing-shan, et al. Microscopic characterization of intra-pore structures of calcareous sands[J]. Rock and Soil Mechanics, 2014, 35(7): 1831−1836.

[4] LÜ Ya-ru, WANG Chong, HUANG Hou-xu, et al. Study on particle structure and crushing behaviors of coral sand[J]. Rock and Soil Mechanics, 2021, 42(2): 352−360.

[5] LV Y, LI X, FAN C, et al. Effects of internal pores on the mechanical properties of marine calcareous sand particles[J]. Acta Geotechnica, 2021, 16: 3209−3228.

[6] CHEN B, HU J M. Fractal behavior of coral sand during creep[J]. Frontiers in Earth Science, 2020, 8:134.

[7] WANG Yi-qun, HONG Yi, GUO Zhen, et al. Micro-and macro-mechanical behavior of crushable calcareous sand in South China Sea[J]. Rock and Soil Mechanics, 2018, 39(1): 199−206+215.

[8] WU Yang, CUI Jie, LI Neng, et al. Experimental study on the mechanical behavior and particle breakage characteristics of hydraulic filled coral sand on a coral reef island in the South China Sea[J]. Rock and Soil Mechanics, 2020, 41(10): 3181−3191.

[9] EDWARD A, DIJKSTRA J, ROUBIN E, et al. A peek into the origin of creep in sand[J]. Granular Matter, 2019, 21(11): 1−8.

[10] LIANG Yu, GU Kai, WU Jing-hong, et al. A study on evolution of aquifer creep potential based on mesoscopic characteristics[J/OL]. Journal of Engineering Geology, 2021. DOI: 10.13544/j.enki.jep.2020-253.

[11] SANZENI A, WHITTLE A J, GERMAINE J T, et al. Compression and creep of Venice lagoon sands[J]. Journal of Geotechnical and Geoenvironmental Engineering, 2012, 138(10): 1266−1276.

[12] LÜ Y, LI F, LIU Y, et al. Comparative study of coral sand and silica sand in creep under general stress states[J]. Canadian Geotechnical Journal, 2016, 54(11): 1601−1611.

[13] WANG Y S, MA L J, WANG M Y, et al. A creep constitutive model incorporating deformation mechanisms for crushable calcareous sand[J]. Arabian Journal of Geosciences, 2018(623): 1−8.

[14] LADE P V, LIGIO JRCD, NAM J. Strain rate, creep, and stress drop-creep experiments on crushed coral sand[J]. Journal of Geotechnical and Geoenvironmental Engineering, 2009, 135(7): 941−953.

[15] LADE P V, NAM J, LIGIO J. Effects of particle crushing in stress drop-relaxation experiments on crushed coral sand[J]. Journal of Geotechnical and Geoenvironmental Engineering (ASCE), 2010, 136(3): 500−509.

[16] ZHANG Xiao-yan, CAI Yan-yan, WANG Zhen-bo, et al. Fractal breakage and particle shape analysis for coral sand under high-pressure and one-dimensional creep conditions[J]. Rock and Soil Mechanics, 2018, 39(5): 1573−1580.

[17] WANG J, FAN P, WANG M, et al. Experimental study of one-dimensional compression creep in crushed dry coral sand[J]. Canadian Geotechnical Journal, 2020, 57(12): 1854−1869.

[18] XIAO Y, YUAN Z, DESAI C, et al. Effects of load duration and stress level on deformation and particle breakage of carbonate sands[J]. International Journal of Geomechanics, 2020, 20(7): 06020014.

[19] COOP M R, SORENSEN K K, BODAS FREITAS T, et al. Particle breakage during shearing of a carbonate sand[J]. Géotechnique, 2004, 54(3): 157−163.

[20] SHEN C M, YU J D, LIU S H, et al. A unified fractional breakage model for granular materials inspired by the crushing tests of dyed gypsum particles[J]. Construction and Building Materials, 2021, 270: 121366.

[21] MIAO G, AIREY D. Breakage and ultimate states for a carbonate sand[J]. Géotechnique, 2013, 63(14): 1221−1229.

[22] ZHANG X, HU W, SCARINGI G, et al. Particle shape factors and fractal dimension after large shear strains in carbonate sand[J]. Géotechnique Letters, 2018, 8(1): 73−79.

[23] ZHANG Ji-ru, ZHANG Bi-wen, HU Yong, et al. Predicting the particle breakage of granular geomaterials[J]. Chinese Journal of Rock Mechanics and Engineering, 2016, 35(9): 1898−1905.

[24] EINAV I. Breakage mechanics-part Ⅰ: theory[J]. Journal of the Mechanics and Physics of Solids, 2007, 55(6): 1274−1297.

[25] Ministry of Water Resources of the People's Republic of China. GB/T50123 — 2019 Standard for soil test method[S]. Beijing: China Planning Press, 2019.

[26] TONG Chen-xi, ZHANG Sheng, LI Xi, et al. Evolution of geotechnical materials based on Markov chain considering particle crushing[J]. Chinese Journal of Geotechnical Engineering, 2015, 37(5): 870−877.

[27] LIN Lan, LI Sa, SUN Li-qiang, et al. Study on evolution of particle breakage of carbonate soils based on fractal theory[J]. Chinese Journal of Rock Mechanics and Engineering, 2021, 40(3): 640−648.

[28] YANG Dian-sen, CHEN Wei-zhong, YANG Jian-ping, et al. Experimental study of micro-macro damage properties of rock salt during creep test by means of digital image correlation technique[J]. Chinese Journal of Rock Mechanics and Engineering, 2011, 30(7): 1363−1367.

[29] WANG W, COOP M R. An investigation of breakage behavior of single sand particles using a high-speed microscope camera[J]. Géotechnique, 2016, 66(12): 1−15.

[30] LI H Y, CHAI H W, XIAO X H, et al. Fractal breakage of porous carbonate sand particles: microstructures and mechanisms[J]. Powder Technology, 2020, 363: 112−121.

[31] LEE C, SUH H S, YOON B, et al. Particle shape effect on thermal conductivity and shear wave velocity in sands[J]. Acta Geotechnica, 2017, 12(3): 615−625.

[32] SHEN Yang, SHEN Xue, YU Yan-ming, et al. Macro-micro study of compressive deformation properties of calcareous sand with different particle fraction contents[J]. Rock and Soil Mechanics, 2019, 40(10): 3733−3740.

[33] ZHANG Bin, CHAI Shou-xi, WEI Hou-zhen, et al. Influence of coral sand particle shape on the compression property of coarse grained calcareous soil[J]. Journal of Engineering Geology, 2020, 28(1): 85−93.

[34] CHEN Hai-yang, WANG Ren, LI Jian-guo, et al. Grain shape analysis of calcareous soil[J]. Rock and Soil Mechanics, 2005, 26(9): 1389−1392.

[35] KUANG D M, LONG Z L, GUO R Q, et al. Experimental and numerical investigation on size effect on crushing behaviors of single calcareous sand particles[J]. Marine Georesources & Geotechnology, 2020, 39(5).

[36] TYLER S W, WHEATCRAFT S W. Fractal scaling of soil particle-size distributions: analysis and limitations[J]. Soil Science Society of America Journal, 1992, 56(2): 362−369.

[37] YE Wan-jun, WU Yun-tao, YANG Geng-she, et al. Study on microstructure and macro-mechanical properties of paleosol under dry-wet cycles[J]. Chinese Journal of Rock Mechanics and Engineering, 2019, 38(10): 2126−2137.

[33] ZHAO B, WANG J, COOP M R, et al. An investigation of single sand particle fracture using X-ray micro-tomography[J]. Géotechnique, 2015, 65(8): 625−641.